GEOPHYSICAL RESEARCH LETTERS, VOL. 33, L19706, doi:10.1029/2006GL026821, 2006

Climate change and interannual variability of precipitation in South America

Alice M. Grimm[1] and Angela A. Natori[1]

Received 5 May 2006; revised 6 July 2006; accepted 18 August 2006; published 7 October 2006.

[1] We analyze the interannual variability of the summer monsoon rainy season in South America and its relationship with SST as simulated by the ocean-atmosphere coupled model ECHAM5-OM for present-day conditions (1961–1990) and future A2 emission scenario (2071–2100). The first mode of model precipitation variability, both in spring and summer, is associated with El Niño-Southern Oscillation (ENSO). In both seasons it features a dipole of anomalies between northern and southeastern South America. These modes correspond, with some differences, to the first variability mode of observed spring precipitation, and to the third variability mode of observed summer precipitation, which are also associated with ENSO. The relationship between ENSO events and precipitation variability in southeastern South America weakens for the A2 scenario, especially in spring, which is presently the season with strongest ENSO-related impact. The weakened teleconnection is probably due to the reduction of the SST subtropical latitudinal gradient in the ENSO mode.
Citation: Grimm, A. M., and A. A. Natori (2006), Climate change and interannual variability of precipitation in South America, *Geophys. Res. Lett.*, *33*, L19706, doi:10.1029/2006GL026821.

1. Introduction

[2] An important aspect of the possible effects of climate change associated with increasing concentrations of greenhouse-gases in the atmosphere is the impact on precipitation variability and its relationships with sea surface temperature anomalies (SST). South American precipitation is strongly affected by El Niño-Southern Oscillation (ENSO) episodes [e.g., *Ropelewski and Halpert*, 1987; *Aceituno*, 1988; *Grimm et al.*, 2000; *Grimm*, 2003, 2004], both in the tropics and extratropics. Therefore, it is interesting to verify how a state-of-the-art ocean-atmosphere coupled general circulation model used to project future climate for the IPCC Assessment Report 4 reproduces the main aspects of that variability and its relationships with SST in present-day simulations, and what are the projected changes in the ENSO-precipitation relationship. These aspects have not been addressed yet for South America (SA). The analysis will focus on austral spring (SON) and summer (DJF), which are important periods within the South American summer monsoon season. The variability of this season is of utmost importance for agriculture, reservoir management, and natural disaster preparedness, for this is the peak rainy season in most of the continent, including very populous regions.

2. Model, Data, and Methods

[3] Present day simulations (1961–1990) and future climate projections (2071–2100) assuming the SRES A2 emission scenario [*Intergovernmental Panel on Climate Change*, 2000] are provided by state-of-the-art ocean-atmosphere coupled general circulation model ECHAM5-OM [*Roeckner et al.*, 2003; *Marsland et al.*, 2003; *Latif et al.*, 2004], with resolution $1.875° \times 1.875°$. This model showed one of the best performances in reproducing El Niño-Southern Oscillation (ENSO) in a recent assessment of models that contribute with future climate projections for the IPCC-Assessment Report 4 [*Oldenborgh et al.*, 2005]. Besides, it shows a comparatively good simulation of the present-day SA precipitation climatology (figures not shown). A three-member ensemble mean is used in this analysis.

[4] The validation of the models' performance is carried out by comparing the models' precipitation variability with that obtained from the University of Delaware data set [*Legates and Willmott*, 1990]. The variability is characterized by Empirical Orthogonal Functions (EOFs) and its connection with SST anomalies is assessed through correlation analysis of the corresponding factor scores series with SST. The SST data for correlation with observed precipitation variability are provided by the HadISST1 reconstruction of observed global sea surface temperature [*Rayner et al.*, 2003], while the models' precipitation variability is correlated with the SST output of the model itself. An EOF analysis was also carried out of the model SST for the two periods analyzed in order to test some hypotheses concerning the changing relationship between SA precipitation and ENSO.

3. Results

[5] The main feature of the first mode of precipitation variability in the model, both in spring and summer, is a north-south dipole of anomalies (Figures 1 and 2). In both seasons it is significantly associated with El Niño-Southern Oscillation (ENSO), as shown by the correlation maps with SST. It explains 20.7% of the variance in spring and 22.1% in summer.

[6] The important role of ENSO in the interannual variability of observed precipitation in spring is confirmed by its first EOF, which is also connected with ENSO (Figure 3). However, it explains less variance (14.9%) than in the model. This mode of observed precipitation also features a dipole, but the northern center is over northeast-

[1]Department of Physics, Federal University of Paraná, Curitiba, Brazil.

0094-8276/06/2006GL026821$05.00

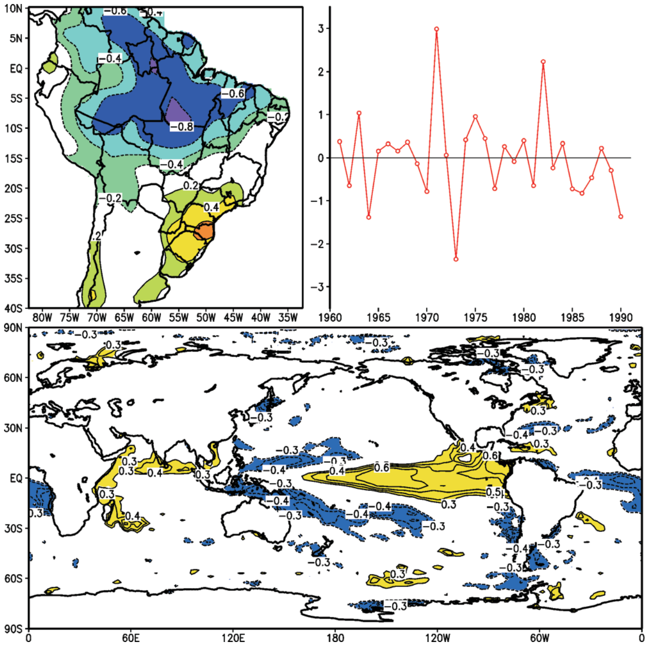

Figure 1. (top) Factor loadings and factor scores of the first EOF of simulated spring precipitation in the period 1961–1990, and (bottom) correlation coefficients between factor scores and SST. Correlation coefficients significant to a level better than 0.05 in a one-sided student's t-test are shaded clear (positive) and dark (negative). This mode explains 20.7% of the variance.

ern SA, while the maximum variability in the model is extended westward, over central Amazonia (compare Figures 1 and 3). The southern center is placed over southeastern SA, both in nature and in the model. The impact of ENSO events on this region in spring is strong and consistent [e.g., *Grimm et al.*, 2000; *Grimm*, 2003, 2004]. As would be expected, the series of factor scores for the model data (Figure 1) does not reproduce closely the series for observed data (Figure 3), in which known El Niño (La Niña) events correspond to positive (negative) values. This means that the model reproduces an ENSO-like variability but does not forecast correctly the occurrence of particular ENSO events. There is a good correspondence between the correlation maps of SST with the factor scores of the first precipitation EOF in nature and in the model.

[7] Differently from spring, the first variability mode of observed summer precipitation is not related with ENSO (not shown). The observed mode with greater similarity to the first mode of summer precipitation in the model is the third mode, which is also associated with ENSO but only explains 9.9% of the variance (Figure 4). This shows that in summer the model overestimates the influence of ENSO even more than in spring. As a matter of fact, diagnostic studies indicate that regional processes might be more important for the interannual variability of summer precipitation than remote processes [*Grimm*, 2003, 2004]. The model does not seem to reproduce these processes, as the ENSO-related mode explains 22.1% of the model summer precipitation variance. The stronger atmospheric response to ENSO in the models, when compared to observations, has been reported in some studies [e.g., *Peng et al.*, 2000;

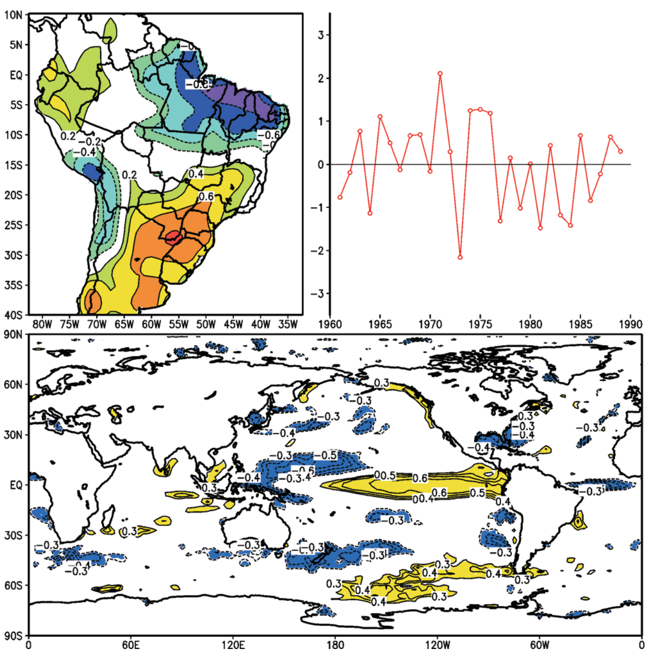

Figure 2. (top) Factor loadings and factor scores of the first EOF of simulated summer precipitation in the period 1961–1990, and (bottom) correlation coefficients between factor scores and SST. Correlation coefficients significant to a level better than 0.05 in a one-sided student's t-test are shaded clear (positive) and dark (negative). This mode explains 22.1% of the variance.

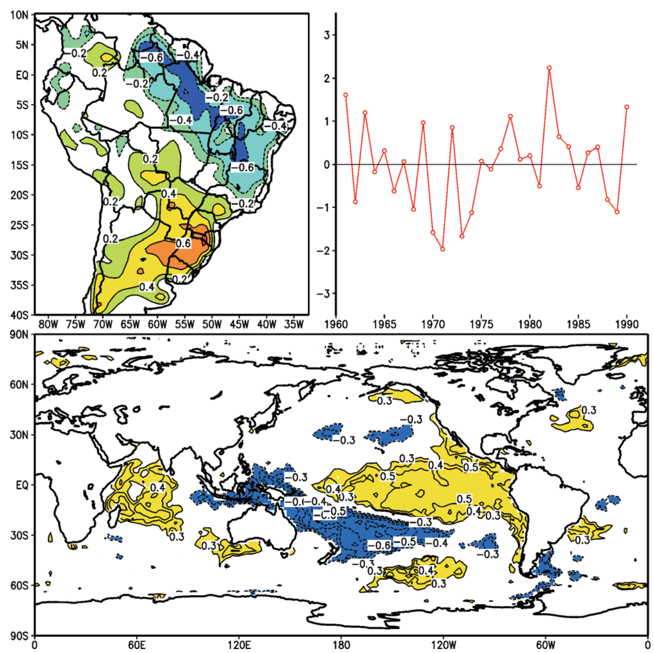

Figure 3. (top) Factor loadings and factor scores of the first EOF of observed spring precipitation in the period 1961–1990, and (bottom) correlation coefficients between factor scores and SST. Correlation coefficients significant to a level better than 0.05 in a one-sided student's t-test are shaded clear (positive) and dark (negative). This mode explains 14.9% of the variance.

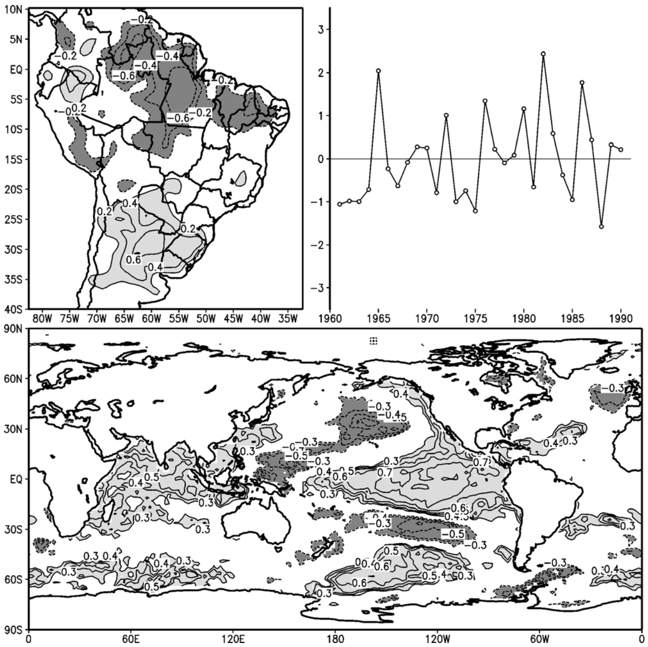

Figure 4. (top) Factor loadings and factor scores of the third EOF of observed summer precipitation in the period 1961–1990, and (bottom) correlation coefficients between factor scores and SST. Correlation coefficients significant to a level better than 0.05 in a one-sided student's t-test are shaded clear (positive) and dark (negative). This mode explains 9.9% of the variance.

Grimm et al., 2006]. The significant correlation with SST anomalies in the tropical eastern Pacific Ocean is confined within a rather narrow equatorial region (Figure 2), while the correlation between observed precipitation variability and SST extends into the subtropics (Figure 4). The relationship between precipitation over Northeast Brazil and SST in southern equatorial Atlantic, included in the first model variability mode (Figure 2), is not evident in the corresponding ENSO-related variability mode of the observed summer precipitation (Figure 4). That relationship is described in a separate mode of observed precipitation (not shown).

[8] The enhanced emission scenario modifies the spatial pattern of the first variability mode of spring precipitation by enhancing and enlarging the northern center of the dipole and weakening the southern center (compare Figures 1 and 5). This mode explains 26.4% of the variance, which is higher than the variance explained by the first mode of the present-day precipitation variability. The correlation between this mode and SST under A2 scenario is weaker in eastern equatorial Pacific (although still significant), but the significant correlation extends into the subtropics (Figure 5).

[9] The impact of ENSO over SA precipitation is exerted through perturbation of the Walker circulation over Amazonia and through anomalous Rossby wave propagation from eastern Pacific towards southeastern SA [e.g., *Souza and Ambrizzi*, 2002; *Grimm*, 2003, 2004]. The stronger variability components over Amazonia in the climate change scenario might be produced by enhanced anomalies of Walker circulation associated with the broader area showing significant correlation with SST in the tropical central-eastern Pacific (Figure 5). The westward shift of the northern center of precipitation anomalies might be associated with the strengthening of the ENSO-related SST anomalies over the equatorial central Pacific (Figure 5), when compared to the correlations with present-day SST anomalies (Figure 1). On the other hand, the weakening of the relationship with southeastern SA can be attributed to the reduction of the SST latitudinal gradient in subtropical South Pacific (compare Figures 1 and 5). The sea surface temperature anomalies at the subtropical south-central Pacific and the enhancement of the SST latitudinal gradient in central-eastern South Pacific during El Niño events are important features associated with the impact of these events on the spring precipitation variability in southeastern SA [*Barros and Silvestri*, 2002; *Vera et al.*, 2004]. El Niño events in which this gradient was weak did not produce significant impact on the region. This gradient contributes to the enhancement of the subtropical jet and favors Rossby wave propagation from the tropical central-east Pacific towards southeastern SA, producing circulation anomalies that enhance precipitation [*Grimm*, 2003].

[10] The EOF analysis of the present and future SSTs from the model supports these hypotheses on the changing ENSO teleconnection. The first mode (not shown) indicates a clear tendency to increasing SSTs over all the oceanic basins under the A2 scenario, but with less intensity in the equatorial central-eastern Pacific if compared with the subtropical latitudes, implying a weaker latitudinal SST gradient. The weakening of the tropical-subtropical SST

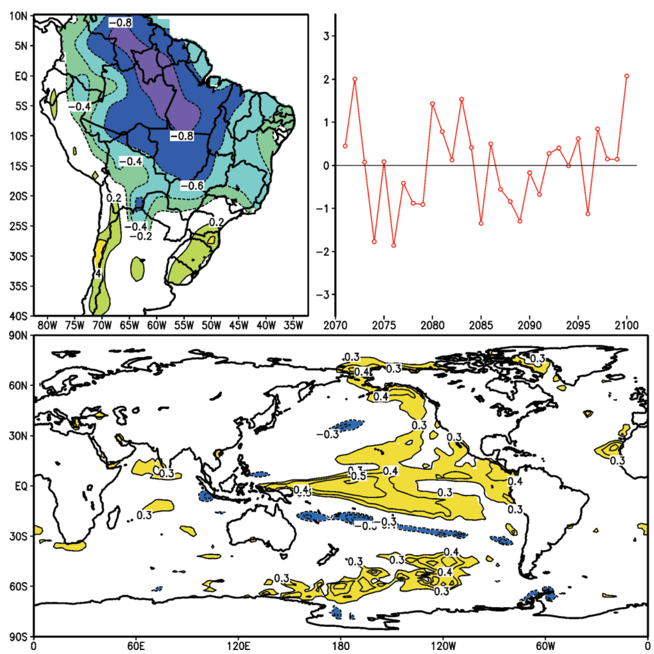

Figure 5. (top) Factor loadings and factor scores of the first EOF of simulated spring precipitation in the period 2071–2100, assuming the A2 emission scenario, and (bottom) correlation coefficients between factor scores and SST. Correlation coefficients significant to a level better than 0.05 in a one-sided student's t-test are shaded clear (positive) and dark (negative).

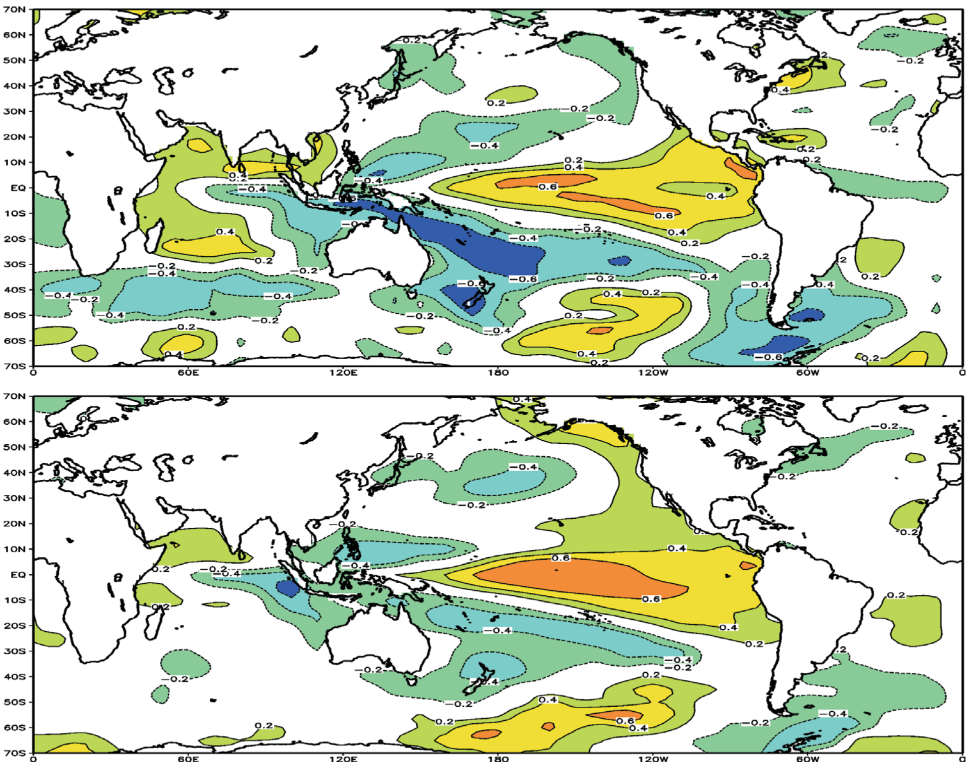

Figure 6. Factor loadings of the second variability mode of SSTs simulated by ECHAM5-OM for spring (SON) during the period (top) 1961–1990 and (bottom) 2071–2100.

gradient in central-east Pacific from the present to future climate is also evident in the second mode, which represents ENSO-related variability (compare Figure 6 (top) and Figure 6 (bottom)), and the reduction is even stronger near SA. The SST anomalies in the tropical central Pacific are slightly stronger in the future climate than in present-day conditions. This SST mode, in both periods, is strongly correlated with the first variability mode of precipitation (represented in Figures 1 and 5).

[11] The first summer precipitation variability mode under A2 scenario explains 21.1% of the variance and also shows enhancement and westward shift of the northern center and weakening of the southern center with respect to the present-day conditions (Figure 7). Some of the changes in the relationship with SST reported for spring are also observed in summer, but with less intensity. The factor scores series shows clearly a negative tendency, contrary to spring. This means a tendency to more precipitation in Amazonia in summer, consistently with the climate change in 2071–2100 projected by this model (figure not shown).

[12] Another outstanding feature of the correlation patterns between SST and the factor scores series of EOF1 (both for spring and summer) for 2071–2100 is the absence of significant correlations in the tropical Atlantic Ocean, which are present in the period 1961–1990.

4. Conclusions

[13] The first variability modes of observed precipitation and their relationships with SST are well represented in the model, although the importance of ENSO events in gener-

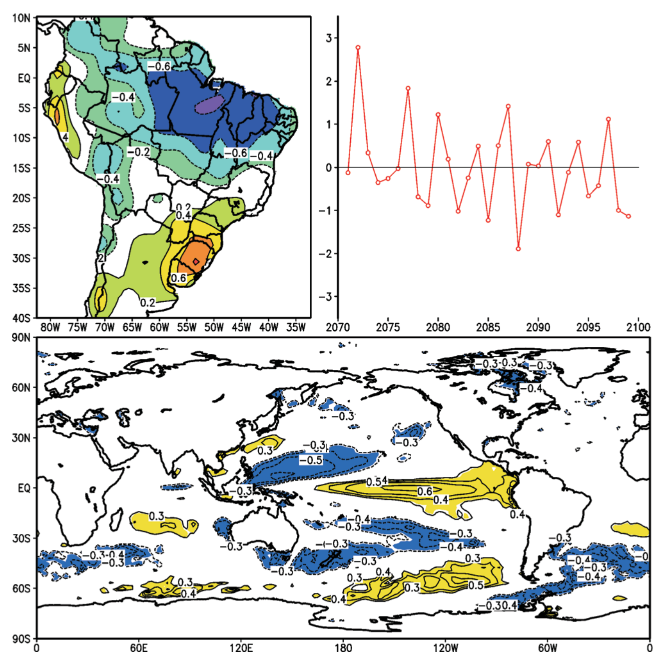

Figure 7. (top) Factor loadings and factor scores of the first EOF of simulated summer precipitation in the period 2071–2100, assuming the A2 emission scenario, and (bottom) correlation coefficients between factor scores and SST. Correlation coefficients significant to a level better than 0.05 in a one-sided student's t-test are shaded clear (positive) and dark (negative).

ating this variability is overestimated in the model, especially in summer. This is a feature also observed in other models.

[14] The enhanced emission scenario reduces the ENSO impact on southeastern SA spring precipitation, which is presently strong and consistent. The contrast between equatorial and subtropical SST anomalies is reduced in central-eastern Pacific and the extratropical SST warming is enhanced in the projected future climate. This feature is associated with a weaker subtropical westerly jet and, therefore, with less favorable conditions for Rossby wave propagation towards southeastern SA, weakening the ENSO teleconnection with this region. On the other hand, the impact on the northern part of SA is enhanced, which is indicated by significant correlation between the first precipitation mode and SST over a broader area in central-east Pacific. The contribution of the first variability mode to the total variance of precipitation is enhanced in spring in the climate change scenario, but it is mainly concentrated in northern SA. These changes would produce great impact on interannual variability of precipitation in southeastern SA, for spring is the rainy season in part of this region.

[15] In summer the projected changes show some similarities to those reported for spring, but they are weaker. The results are consistent with the precipitation changes projected by this model for SA. They indicate that the precipitation change in Amazonia is closely related with the tendency in the ENSO-related variability mode for precipitation.

[16] **Acknowledgments.** This study was supported by MMA-Brazil/PROBIO (GEF and BIRD), Conselho Nacional de Desenvolvimento Científico e Tecnológico (CNPq – Brazil), and Inter-American Institute for Global Change Research (CRN055).

References

Aceituno, P. (1988), On the functioning of the Southern Oscillation in the South American sector. Part I: Surface climate, *Mon. Weather Rev.*, *116*, 505–524.

Barros, V. R., and G. E. Silvestri (2002), The relation between sea surface temperature at the subtropical south-central Pacific and precipitation in southeastern South America, *J. Clim.*, *15*, 251–267.

Grimm, A. M. (2003), The El Niño impact on the summer monsoon in Brazil: Regional processes versus remote influences, *J. Clim.*, *16*, 263–280.

Grimm, A. M. (2004), How do La Niña events disturb the summer monsoon system in Brazil?, *Clim. Dyn.*, *22*(2–3), 123–138.

Grimm, A. M., V. R. Barros, and M. E. Doyle (2000), Climate variability in southern South America associated with El Niño and La Niña events, *J. Clim.*, *13*, 35–58.

Grimm, A. M., A. K. Sahai, and C. F. Ropelewski (2006), Interdecadal variations in AGCM simulation skills, *J. Clim.*, *19*, 3406–3419.

Intergovernmental Panel on Climate Change (2000), Special Report on Emission Scenarios, Working Group III, 20 pp., Geneva, Switzerland. (Available at http://www.ipcc.ch/pub/SPM_SRES.pdf)

Latif, M., et al. (2004), Reconstructing, monitoring, and predicting decadal-scale changes in the North Atlantic thermohaline circulation with sea surface temperature, *J. Clim.*, *17*, 1605–1614.

Legates, R. D., and C. J. Willmott (1990), Mean seasonal and spatial variability in gauge-corrected global precipitation, *Int. J. Climatol.*, *10*, 111–127.

Marsland, S., H. Haak, J. Jungelaus, M. Latif, and F. Röske (2003), The Max-Planck-Institute global ocean/sea ice model with orthogonal curvilinear coordinates, *Ocean Model.*, *5*, 91–127.

Oldenborgh, G. J., S. Philip, and M. Collins (2005), El Niño in a changing climate: A multi-model study, *Ocean Sci. Disc.*, *2*, 267–298.

Peng, P., A. Kumar, A. G. Barnston, and L. Goddard (2000), Simulation skills of the SST-forced global climate variability of the NCEP-MRF9 and the Scripps_MPI ECHAM3 models, *J. Clim.*, *13*, 3657–3679.

Rayner, N. A., D. E. Parker, E. B. Horton, C. K. Folland, L. V. Alexander, D. P. Rowell, E. C. Kent, and A. Kaplan (2003), Global analyses of sea surface temperature, sea ice, and night marine air temperature since the late nineteenth century, *J. Geophys. Res.*, *108*(D14), 4407, doi:10.1029/2002JD002670.

Roeckner, E., et al. (2003), The atmospheric general circulation model ECHAM5. Part I: Model description, *MPI Rep. 349*, Max-Planck-Inst. für Meteorol., Hamburg, Germany.

Ropelewski, C. F., and M. S. Halpert (1987), Global and regional scale precipitation patterns associated with the El Niño/Southern Oscillation, *Mon. Weather Rev.*, *115*, 1606–1626.

Souza, E. B., and T. Ambrizzi (2002), ENOS impacts on the South American rainfall during 1980s: Hadley and Walker circulation, *Atmosfera*, *15*, 105–120.

Vera, C. S., G. Silvestri, V. Barros, and A. Carril (2004), Differences in El Niño response over the Southern Hemisphere, *J. Clim.*, *17*, 1741–1753.

A. M. Grimm and A. A. Natori, Department of Physics, Federal University of Paraná, Curitiba 81531-990, Brazil. (grimm@fisica.ufpr.br)